

RESEARCH ARTICLE

Inhibition of ERK signaling for treatment of ER α positive TNBCDavid Musheyev¹, Esther Miller², Natania Birnbaum², Elisheva Miller², Shoshana Erlich³, Alyssa Schuck², Anya Alayev^{2*}

1 Department of Internal Medicine, Stony Brook Southampton Hospital, Southampton, New York, United States of America, **2** Department of Biology, Stern College for Women, Yeshiva University, New York, New York, United States of America, **3** Department of Mechanical Engineering, Rutgers University, New Brunswick, New Jersey, United States of America

* anya.alayev@yu.edu

OPEN ACCESS

Citation: Musheyev D, Miller E, Birnbaum N, Miller E, Erlich S, Schuck A, et al. (2023) Inhibition of ERK signaling for treatment of ER α positive TNBC. PLoS ONE 18(5): e0283047. <https://doi.org/10.1371/journal.pone.0283047>

Editor: Ming Tan, Institute of Biomedical Sciences, TAIWAN

Received: August 8, 2022

Accepted: February 28, 2023

Published: May 10, 2023

Copyright: © 2023 Musheyev et al. This is an open access article distributed under the terms of the [Creative Commons Attribution License](https://creativecommons.org/licenses/by/4.0/), which permits unrestricted use, distribution, and reproduction in any medium, provided the original author and source are credited.

Data Availability Statement: All relevant data are within the manuscript and its [Supporting information](#) files.

Funding: AA, CA220021, NIH AA, no grant number, Appelbaum foundation. The funders had no role in study design, data collection and analysis, decision to publish, or preparation of the manuscript.

Competing interests: The authors have declared that no competing interests exist.

Abstract

Breast cancer is the second leading cause of cancer-related deaths in women and triple-negative breast cancer (TNBC), in particular, is an aggressive and highly metastatic type of breast cancer that does not respond to established targeted therapies and is associated with poor prognosis and worse survival. Previous studies identified a subgroup of triple-negative breast cancer patients with high expression of estrogen related receptor alpha (ER α) that has better prognosis when treated with tamoxifen. We therefore set out to identify common targets of tamoxifen and ER α in the context of TNBC using phosphoproteomic analysis. In this study, we discovered that phosphorylation of mitogen-activated protein kinase 1 (MAPK1) is regulated by tamoxifen as well as ER α . Additionally, we showed that inhibition of MAPK signaling together with the use of a selective ER α inverse agonist, XCT-790, leads to a significant upregulation of apoptosis and paves way for the therapeutic use of MAPK inhibitors for treatment of ER α expressing TNBC.

Introduction

Breast cancer is one of the most common cancers in women and is the second leading cause of cancer-related deaths in women [1, 2]. The rate at which breast cancer is diagnosed is astonishing, with about a quarter of a million women diagnosed with invasive breast cancer in the United States annually and 1 in 8 women diagnosed within their lifetime [3]. Risk factors such as age, body-mass-index, and ethnicity are confounding factors for developing breast cancer [3–6]. Certain ethnic groups are disproportionately affected by breast cancer with a higher mortality despite a lower incidence, indicating that there remains a lot about this disease that we still do not know [3–5].

Further subclassification of breast cancer based on molecular status of the tumor reveals a correlation between prognosis and receptor expression. Tumors are classified based on expression of the following known molecular markers: estrogen receptor alpha (ER α), progesterone receptor (PR), and human epidermal growth factor receptor 2 (HER2) [5, 7]. ER α expressing tumors account for 70% of breast cancers [8] and carry a better prognosis than triple negative breast cancer (TNBC), classified as tumors that do not express ER α , PR and

no amplification of HER2, which account for 15–20% of breast cancers [5, 9–12]. Unlike ER α expressing tumors, TNBCs tend to affect younger, premenopausal women, have a higher mortality rates of 40% within the first 5 years after diagnosis, and disproportionately affect African Americans [3, 5]. A combination of the poor prognosis in TNBC and predominance in African Americans might be driving the racial disparity of breast cancer survival. Therefore, the difference in prognosis and receptor expression between ER α expressing tumors and TNBCs requires diverging therapeutic approaches in the treatment of the two cancers.

Approaches to treating ER α expressing tumors focus on inhibiting ER α function with endocrine therapies by either antagonizing the binding of estrogen to ER α (selective estrogen receptor modulators), promoting ER α degradation (selective estrogen receptor degraders), or by blocking estrogen synthesis (aromatase inhibitors) [13, 14]. An example of one of the earlier used selective estrogen receptor modulators (SERM) is tamoxifen. Approved by the FDA in 1977, it was found to be most beneficial in tumors with high expression of ER α and continues to be used therapeutically today [14, 15]. Patients respond very well to tamoxifen treatment with 40–50% reduction in both distant and local recurrence with 5 years of treatment [8]. However, new or acquired resistance develops in approximately 30% of cases and tumors can spontaneously convert to hormone-independent proliferation or can lose ER α expression altogether, creating a greater need for understanding molecular mechanisms of hormone receptor negative breast cancer [15–18]. Therefore, further research has focused on identifying alternative molecular pathways responsible for tumor progression as druggable targets [9, 10, 12, 19], and such research overlaps with the search for targeted treatments for TNBCs.

Since TNBC tumors do not express any known markers, treatment options for TNBC patients are extremely limited and currently no targeted therapies exist for such patients [12]. This leaves chemotherapy as the only treatment option for TNBC [11, 12, 20–22] with a three-year overall survival of 74% compared to 89% in non-TNBC tumors, indicating that chemotherapy is not very effective [20]. Besides for leading to a significantly lower survival in ER α negative tumors as compared to ER α expressing tumors, this treatment option burdens patients with the adverse effects of chemo-toxicity such as alopecia, myelosuppression, gastrointestinal disturbances, nephrotoxicity, neurotoxicity, cardiotoxicity, and infertility, calling into question any benefit from chemotherapy at the cost of a reduced quality of life [23]. Current scientific work aims to offer insights into molecular drivers that may be leveraged in the treatment of TNBC by further classifying tumor microenvironment, identifying tumor cellular signatures and mRNA expression profiles [9, 10, 12, 19]. One such molecular driver that is currently explored is estrogen related receptor α (ERR α) [24, 25].

ERR α is an orphan nuclear receptor that is part of the superfamily of transcription factors, which include ERR α , ERR β , ERR γ [26]. ERR α is structurally most similar to ER α and there is an overlap in ER α and ERR α binding to response elements in promoters of genes whose expression they regulate [27]. Despite their homology, ligands, such as estrogen, that bind to ER α do not bind to ERR α , therefore signaling between the two molecules is quite divergent [27]. Though its function in metabolic processes in the muscle heart and liver has been described, its role in tumorigenesis is not fully understood [28–32]. Metabolic functions that are regulated or that are thought to influence ERR α include glycolysis, cholesterol metabolism, fatty acid oxidation, and oxidative metabolism [28, 31]. In breast cancer, ERR α expression is mutually exclusive with ER α expression and is correlated with a more aggressive and metastatic disease [27]. Previous studies have shown that although ERR α was a negative predictive marker for progression free survival and disease recurrence, in TNBC-basal-like tumors, when treated with tamoxifen, ERR α expression was associated with a slightly prolonged distal

metastasis-free survival, while those treated with chemotherapy alone, had significantly shorter interval to metastasis. Additionally, patients with elevated nuclear expression of ER α who were treated with tamoxifen had a better prognosis than patients with elevated nuclear ER α who were not treated with tamoxifen, indicating that there is a therapeutic benefit to treating ER α -expressing TNBC patients with tamoxifen and that the action of tamoxifen in TNBCs is ER α dependent [25]. These findings indicated that a subgroup of ER α -negative patients respond to tamoxifen and this effect is dependent on ER α expression. This evidence prompted our current study, whose aim was to investigate the relationship between ER α and tamoxifen in the context of TNBC. To investigate this relationship, phosphoproteomic analysis was performed in TNBC cells to identify common pathways that are regulated by both tamoxifen as well as XCT-790, an inverse agonist of ER α [33] and to identify therapeutic targets. Our findings identify MAPK1 (also known as ERK2) as a common target for tamoxifen and ER α and show that treatment of TNBC cells with a MEK1/2 inhibitor together with XCT-790 leads to activation of apoptosis and inhibition of cell migration and invasion, suggesting that ERK is a potential novel therapeutic target that should be considered for TNBC treatment.

Materials and methods

Cell culture and treatments

MDA-MB-231, MDA-MB-436, MDA-MB-157, Hs 578T, BT-549 sh-control and sh-ER α cells were grown in Dulbecco's modified Eagle's medium (Gibco) with 10% fetal bovine serum (R&D, a Bio-Techne Brand) and 1% penicillin-streptomycin (Gibco). Cells were cultured in a 37°C incubator with a humidified 5% CO₂ atmosphere. MDA-MB-231, MDA-MB-436, MDA-MB-157, Hs 578T, BT-549 cells were purchased from ATCC. sh-ER α and sh-control cells were a kind gift from Dr. Marina Holz.

Cells were treated with either 100 nM tamoxifen in ethanol (Millipore), 10 μ M U0126 in DMSO (Tocris, a Bio-Techne Brand), or 10 μ M XCT-790 in DMSO (Tocris, a Bio-Techne Brand), alone or in combination.

Immunoblotting

Following treatment, cells were lysed in ice cold lysis buffer (RIPA buffer with Triton[®] X-100, Halt[™] Protease & Phosphatase Single-Use Inhibitor Cocktail (100X), ThermoScientific). Insoluble materials were centrifuged out at 14,000 rpm and 4°C for 10 min. Using the Bradford assay (Coomassie Protein Assay Reagent, ThermoScientific) and the Eppendorf Bio-Photometer, cell protein concentrations were measured and normalized. 4X LDS Sample Buffer (Invitrogen B0008) and Bolt[™] 10x Sample Reducing Agent (Invitrogen) were added to the samples followed by denaturation for 10 minutes at 70°C. Samples were resolved through electrophoresis using NuPage[™] 4–12% Bis-Tris Gels (Invitrogen) and then transferred onto a nitrocellulose membrane (ThermoScientific) for staining. Immunoblots were detected using the following primary antibodies: ER α #13826, Phospho-p44/42 MAPK (ERK1) (Tyr204)/ (ERK2) (Tyr187) #5726, Phospho-p90RSK1 (Ser380) #12032, RSK1 #8408, p44/42 MAPK (ERK1/2) #4695, Phospho-MAPK Substrates Motif [PXpTP] MultiMab[™] #14378, Phospho-mTOR (Ser2448) #5536, PARP #9532, and β -Actin #4970. All primary antibodies were ordered from Cell Signaling Technology. After staining with primary antibodies, nitrocellulose membranes were treated with IRDye conjugated secondary antibodies (IRDye[®] 680RD Donkey anti-Mouse IgG Secondary Antibody, IRDye[®] 800CW Goat anti-Rabbit IgG Secondary Antibody, Li-COR), and then imaged using the Odyssey-Clx Li-COR infrared detection instrument. Quantification of immunoblots was performed using Image Studio 5.2 (Li-COR).

Immunoprecipitation assay

Cells were lysed in ice cold IP lysis buffer (Pierce™ IP Lysis Buffer, Halt™ Protease & Phosphatase Single-Use Inhibitor Cocktail (100X), Thermo Scientific). Lysates were subjected to immunoprecipitation with either Sepharose® Bead Conjugated p44/42 MAPK (Erk1/2) antibody #5736 (Cell Signaling Technology) or Protein A Agarose beads, 50% slurry (EMD Millipore) overnight at 4°C. Beads were pelleted from solution, washed twice with IP buffer and once with PBS and boiled using Invitrogen's LDS Sample Buffer and Reducing Agent according to manufacturer's instructions.

Phosphoproteomics sample processing and data analysis

Cells were lysed in RIPA lysis buffer, the supernatant was collected following centrifugation at 21000xg for 10 min, and an acetone precipitation was performed overnight at -20°C. The samples were re-suspended in 7 M urea, reduced with 5 mM DTT (dithiothreitol) and alkylated with 15 mM CAA (chloroacetamide). A standard tryptic digest was performed overnight at 37°C. Solid Phase Extraction (SPE) was then performed using C18 Prep Sep™ cartridges (Waters, WAT054960), followed by reconstitution in 0.5% TFA (trifluoroacetic acid). The SPE cartridge was washed with conditioning solution (90% methanol with 0.1% TFA), and equilibrated with 0.1% TFA. The sample was passed (1 drop/sec) through the equilibrated cartridge, then desalted. The sample was then eluted (1 drop/sec) with an elution solution (50% ACN (acetonitrile) with 0.1% TFA. The sample was then TMT labeled according to kit specifications (ThermoFisher Scientific, 90110), with the exception that labeling was performed for 6hrs instead of 1 hr. Following labeling, another SPE was performed, as stated above. Phosphopeptide enrichment using Titansphere Phos-TiO Kit (GL Sciences, 5010–21312) was then performed. Briefly, samples were reconstituted in 100 μ L of Buffer B (75% ACN, 1% TFA, 20% lactic acid–solution B in the kit). The tip was conditioned by centrifugation with 100 μ L of Buffer A (80% ACN, 1% TFA), followed by conditioning with Buffer B (3000xg, 2min). The samples were then loaded onto the tip and centrifuged twice (1000xg, 5min). The tip was then washed with 50 μ L of Buffer B, followed by 2 washes with 50 μ L of Buffer A (1000xg, 2min). The samples were eluted with 100 μ L of elution 1 (20% ACN, 5% NH₄OH) then 100 μ L of elution 2 (20% ACN, 10% NH₄OH) (1000xg, 5min). A final clean-up step was performed using C18 Spin Columns (Pierce, 89870).

Mass spectrometry, data filtering, and bioinformatics

Mass spectrometry analysis was carried out as follows: to separate peptides, reverse-phase nano-HPLC was performed by a nanoACQUITY UPLC system (Waters Corporation). Peptides were trapped on a 2 cm column (Pepmap 100, 3 μ M particle size, 100 Å pore size), and separated on a 25cm EASYspray analytical column (75 μ M ID, 2.0 μ m C18 particle size, 100 Å pore size) at 45°C. The mobile phases were 0.1% formic acid in water (Buffer A) and 0.1% formic acid in acetonitrile (Buffer B). A 180-minute gradient of 2–30% buffer B was used with a flow rate of 300 nl/min. Mass spectral analysis was performed by an Orbitrap Fusion Lumos mass spectrometer (ThermoFisher Scientific). The ion source was operated at 2.4kV and the ion transfer tube was set to 275°C. Full MS scans (350–2000 m/z) were analyzed in the Orbitrap at a resolution of 120,000 and 4e5 AGC target. The MS2 spectra were collected using a 0.7 m/z isolation width and analyzed by the linear ion trap using 1e4 AGC target after HCD fragmentation at 30% collision energy with 50ms maximum injection time. The MS3 scans (100–500 m/z) were acquired in the Orbitrap at 50,000 resolution, with a 1e5 AGC, 2 m/z MS2 isolation window, at 105ms maximum injection time after HCD fragmentation with a normalized

energy of 65%. Precursor ions were selected in 400–2000 m/z mass range with mass exclusion width of 5–18 m/z. Polysiloxane 371.10124 m/z was used as the lock mass.

The raw mass spectrometry data was searched with MaxQuant (1.6.6.0). Search parameters were as follows: specific tryptic digestion, up to 2 missed cleavages, a static carbamidomethyl cysteine modification, variable protein N-term acetylation, and variable phospho(STY) as well as methionine oxidation using the human UniProtKB/Swiss-Prot sequence database (Downloaded Feb 1, 2017). MaxQuant data was deposited to PRIDE/Proteome Xchange.

Fractionation

Following treatment, MDA-MB-231 cells were harvested, and using NE-PER™ Nuclear and Cytoplasmic Extraction Reagents (ThermoScientific), nuclear fractionation was performed according to manufacturer's instructions.

Cell proliferation assays

Cells were seeded in replicates of 6, at a density of 2,500 cells/well in 96 well plates and allowed to attach overnight. Next day, media were changed to assay media, supplemented with or without agents as indicated. Cell proliferation was assayed after 6 days using the supravital dye neutral red (NR) incorporation. The medium was removed, 0.2 ml of medium containing 0.04 mg/ml NR was added per well, and incubation was continued for 30 min at 37°C. Cells were then rapidly washed and fixed with a 0.2-ml solution of 0.5% formalin, 1% CaCl₂ (v/v), and the NR incorporated into the viable cells was released into the supernatant with a 0.2-ml solution of 1% acetic acid, 50% ethanol. Absorbance was recorded at 540 nm with a microtiter plate spectrophotometer. Experiments were performed a minimum of three times. Cytotoxicity graphic data were presented as the mean percentages of control ± standard deviation (STDEV).

Wound healing assay

Cells were seeded in 6-well plates in complete DMEM media, supplemented with 10% FBS and grown to confluency in monolayer overnight. Wound/scratch was created along the diameter of each well using a 200µl pipette tip. Cell debris were removed by washing once with PBS, followed by addition of fresh DMEM media supplemented with 1% FBS, with or without agents as indicated. Cell imaging and migration were measured using Keyence BZX-800 microscope. Data was analyzed and plotted using Excel. Experiments were performed a minimum of three times.

Boyden chamber assay

Cells were cultured in media without serum and treated with either XCT-790, tamoxifen and/or U0126, as indicated. Nineteen hours later, 1×10^5 cells per well were plated on tissue culture inserts with 8.0-µm pores. The inserts were incubated with serum-free media containing 10 µM XCT-790, 100 nM tamoxifen or 10 µM U0126, alone or in combination. Complete media were added to the lower chamber and cells allowed to migrate for 15 hours. After 15 hours, cells remaining on the upper side of the membrane were scraped off, and the cells that had migrated to the lower side of the membrane were fixed in 4% paraformaldehyde. The insert membranes were removed, stained, and mounted on coverslips using DAPI Fluoromount. Images were collected at 10× magnification using Keyence BZX-800 microscope. Nuclei were counted manually, and data were analyzed using two-tailed Student's *t* test and plotted using Excel. Experiments were performed a minimum of three times.

Microscopy

Cells were imaged under phase contrast lens using the Keyence BZX-800 microscope with a 20x objective.

Statistical analysis

All experiments were repeated at least thrice. Data was analyzed using Excel and significance of data was determined using t-tests, where * represents P values <0.05 , ** represents P values <0.01 , and *** represents P values <0.001 .

Results

To identify common targets that are regulated by both tamoxifen as well as ERK α inverse agonist XCT-790 in TNBC, phosphoproteomic analysis was performed on MDA-MB-231 cells (Fig 1A, S1 Fig and S1 Table). Bioinformatic analysis identified 307 unique targets with statistically significant phosphorylation ($P < 0.05$) changes (Fig 1B and S2 Table). Further analysis of the data identified 19 unique phosphosites that were changed in both tamoxifen and XCT-790 treated cells (Table 1). A specific direct target which was of particular interest to us was MAPK1, whose phosphorylation was upregulated on tyrosine 187 (also known as p-ERK Y204/187) upon treatment with tamoxifen as well as with XCT-790. MAPK1 is a member of the Ras/Raf/MEK/ERK signaling pathway that regulates cell cycle progression as well as apoptosis and warrants further study as an important player in TNBC progression.

To validate phosphoproteomic findings, MDA-MB-231 cells were grown in serum-free media for 24 hrs and treated with 100 nM tamoxifen and 10 μ M XCT-790, alone or in combination as indicated and probed with an antibody that recognizes proteins that are phosphorylated at the threonine within the PXPpTP motif, also known as the phospho-MAPK substrate motif (Fig 2). As compared to the untreated control, phosphorylation changes in phospho-MAPK substrate motif [PXPpTP] are readily seen and are indicated by asterisks. In tamoxifen or XCT-790 treated samples, phospho-MAPK substrate changes are seen by 15–30 min post treatment (Fig 2A) and in samples treated with combination of tamoxifen and XCT-790, phospho-MAPK substrate changes are pronounced as early as 5 min post treatment (Fig 2B). Counterstaining of the membrane with an antibody specific for the phosphorylation of MAPK1 on tyrosine 187 (p-ERK Y204/187) showed upregulation in phosphorylation upon treatment with XCT-790 and tamoxifen, alone or in combination. Therefore, western blot analysis validated the phosphoproteomic findings and further showed that XCT-790 and tamoxifen treatments regulate MAPK signaling pathway globally in TNBC. To further validate phosphoproteomic findings and explore the relationship between ERK α , tamoxifen, and ERK in the context of TNBC, MDA-MB-231 cells were grown in serum-free media for 24 hrs and treated with tamoxifen and XCT-790, alone or in combination over a time course of 5, 15, 30 and 60 min (Fig 3). Immunoblotting verified that ERK α inhibition by XCT-790 caused statistically significant upregulation of p-ERK Y204/187 as early as 5, 15 and 30 min post treatment (Fig 3A and 3B). Likewise, tamoxifen treatment caused statistically significant upregulation of p-ERK Y204/187 as early as 5, 15 and 30 min post treatment and similar results were observed in the combination of XCT-790 and tamoxifen treated samples (Fig 3D and 3E). Importantly, statistically significant upregulation of p-RSK1 S380, a direct downstream target of ERK, was observed in XCT-790 and tamoxifen treated samples, alone or in combination (Fig 3A and 3C). This finding validates phosphoproteomic's findings and indicates that MEK/ERK/RSK signaling pathway is regulated by ERK α and tamoxifen in TNBC. Additionally, this effect is specific to the MAPK signaling pathway, as XCT-790 or tamoxifen treatment had no impact on activation of mTOR on S2448 (Fig 3A and 3D). Mammalian target of rapamycin (mTOR)

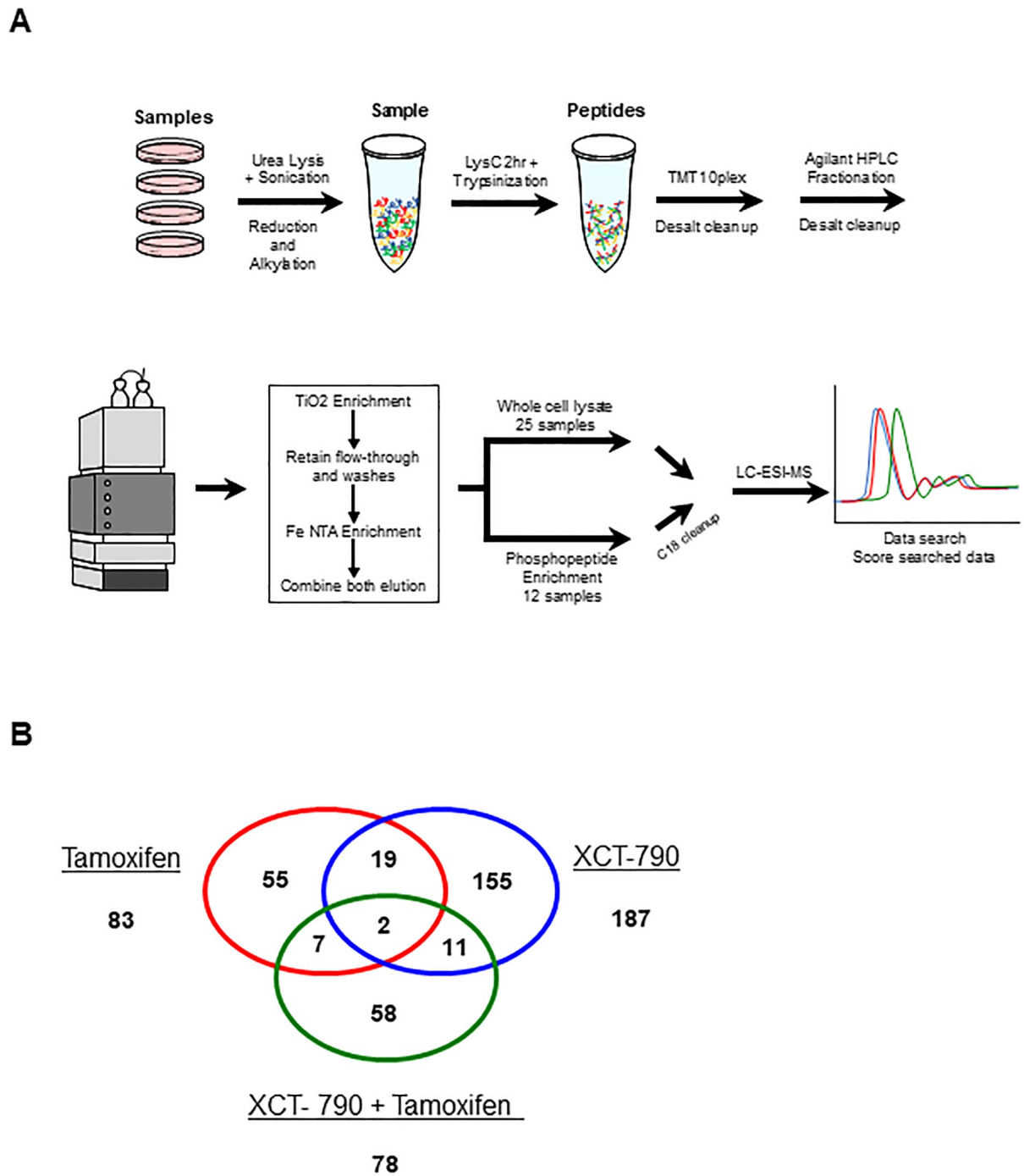


Fig 1. Phosphoproteomic analysis of XCT-790 and tamoxifen treated MDA-MB-231 cells. (A) Steps of the work flow chart of samples treated for the phosphoproteomic analysis. (B) Outcome of number of identified unique phosphorylated proteins in each group.

<https://doi.org/10.1371/journal.pone.0283047.g001>

is a parallel signaling pathway that is activated by growth factors and is often hyperactivated in cancer, including breast cancer [34]. These results indicate that ER α and tamoxifen regulate p-ERK and that this effect is direct and specific to the MAPK signaling pathway.

In an effort to define the relationship between ER α levels and tamoxifen response, as well as to explore the role of ER α in the phosphorylation of ERK, MDA-MB-231 cells with stable

Table 1. Significant phosphoproteomic changes in XCT-790 as well as tamoxifen treated samples. A table of statistically significant hits from phosphoproteomic analysis of cells treated with XCT-790 as well as tamoxifen.

Protein	Protein names	Gene names	Position
Q03252	Lamin-B2	LMNB2	420
Q9Y2U5	Mitogen-activated protein kinase kinase kinase 2	MAP3K2	239
Q08170	Serine/arginine-rich splicing factor 4	SRSF4	431
Q9Y2D5	A-kinase anchor protein 2	AKAP2	720
Q3KQU3-2	MAP7 domain-containing protein 1	MAP7D1	796
Q9BWF3-3	RNA-binding protein 4	RBM4	86
Q9UKV3-5	Apoptotic chromatin condensation inducer in the nucleus	ACIN1	408
Q8WZ73-3	E3 ubiquitin-protein ligase rififylin	RFFL	212
Q5JSH3-2	WD repeat-containing protein 44	WDR44	163
Q13547	Histone deacetylase 1	HDAC1	421
Q96RT1-7	Protein LAP2	ERBB2IP	1015
P42858	Huntingtin	HTT	432
Q13158	FAS-associated death domain protein	FADD	194
Q9NXH8	Torsin-4A	TOR4A	63
Q8IYB3-2	Serine/arginine repetitive matrix protein 1	SRRM1	595
Q9UQ35	Serine/arginine repetitive matrix protein 2	SRRM2	1014
Q8NCF5	NFATC2-interacting protein	NFATC2IP	204
Q15366-7	Poly(rC)-binding protein 2	PCBP2	317
P28482-2	Mitogen-activated protein kinase 1	MAPK1	187

<https://doi.org/10.1371/journal.pone.0283047.t001>

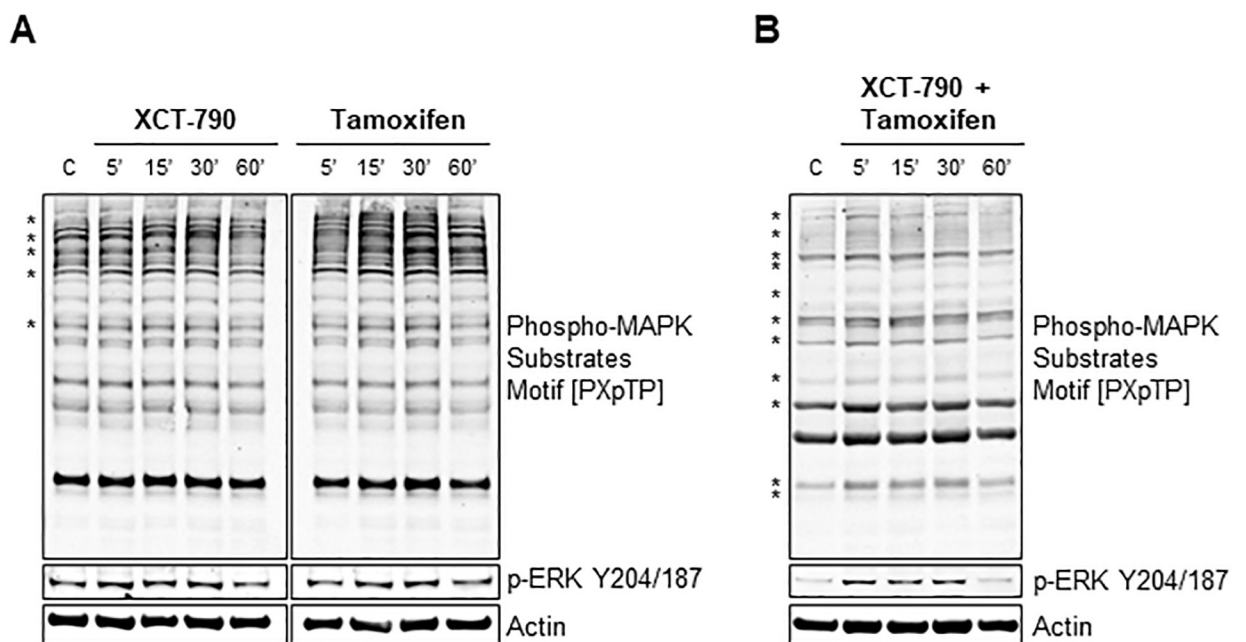


Fig 2. XCT-790 and tamoxifen treatments regulate signaling of MAPK pathway. (A) MDA-MB-231 cells were grown in starvation media for 24 hrs and treated with either 10 μ M XCT-790 or 100 nM tamoxifen for 5, 15, 30 or 60 minutes. Cells were lysed as described in "Materials and Methods" and indicated proteins were detected by immunoblot. (B) MDA-MB-231 cells were grown in starvation media for 24 hrs and treated with 10 μ M XCT-790 and 100 nM tamoxifen for 5, 15, 30 or 60 minutes. Cells were lysed as described in "Materials and Methods" and indicated proteins were detected by immunoblot. * indicates phosphorylation changes in [PXpTP] motif as compared to control. 'C' is untreated control.

<https://doi.org/10.1371/journal.pone.0283047.g002>

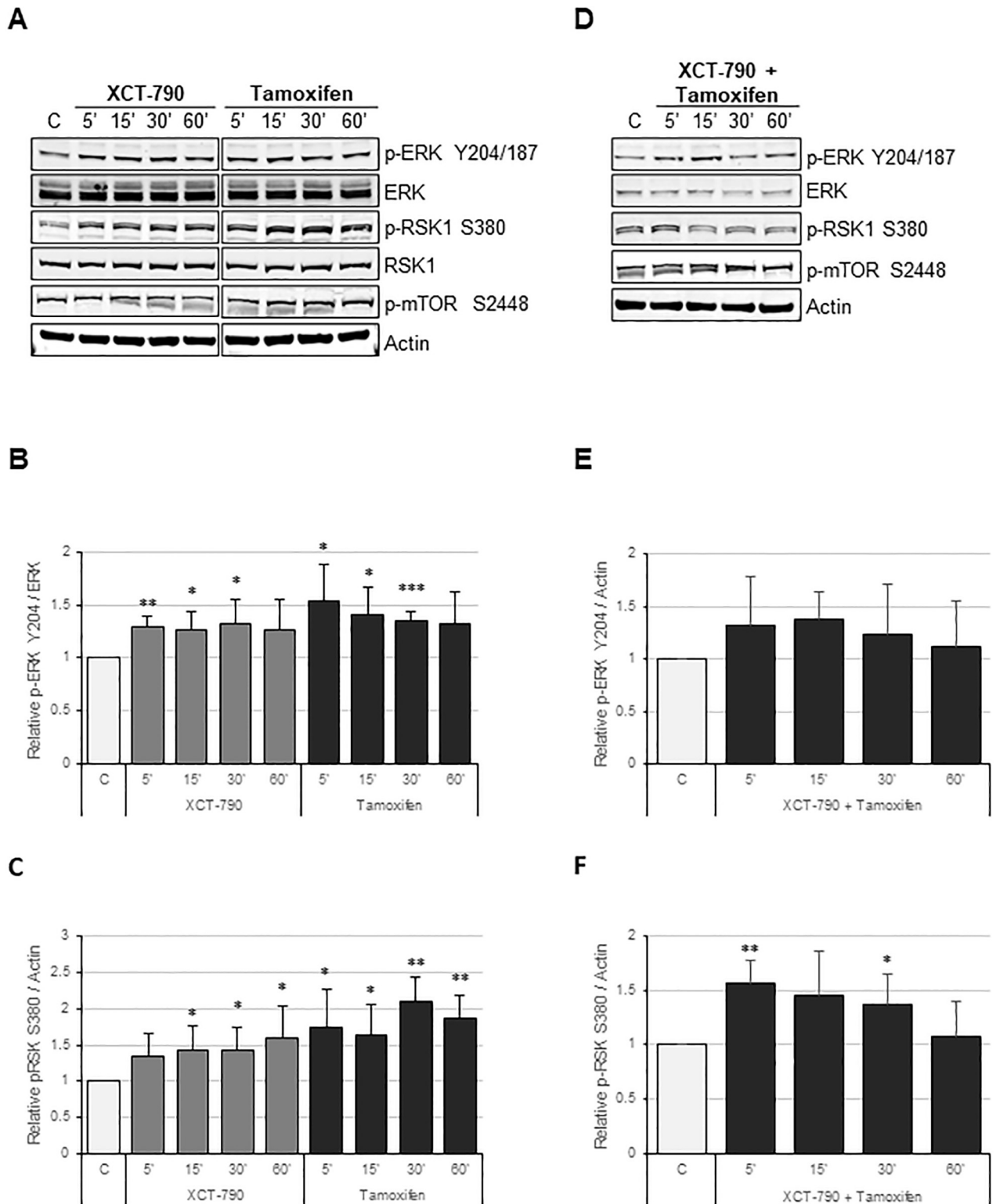


Fig 3. XCT-790 and tamoxifen treatments upregulate phosphorylation of p-ERK on Y204/187. (A) MDA-MB-231 cells were grown in starvation media for 24 hrs and treated with either 10 μ M XCT-790 or 100 nM tamoxifen for 5, 15, 30 or 60 minutes. Cells were lysed as described in “Materials and Methods” and indicated proteins were detected by immunoblot. (B) Quantification of p-ERK Y204/187 protein levels normalized to total ERK signal from ‘A’. (C) Quantification of p-RSK1 S380 protein levels normalized to actin signal from ‘A’. (D) MDA-MB-231 cells were grown in starvation media for 24 hrs and treated with 10 μ M XCT-790 and 100nM tamoxifen for 5, 15, 30 or 60 minutes. Cells were lysed as described in

"Materials and Methods" and indicated proteins were detected by immunoblot. (E) Quantification of p-ERK Y204/187 protein levels normalized to actin signal from 'D'. (F) Quantification of p-RSK1 S380 protein levels normalized to actin signal from 'D'. * represents $P < 0.05$, ** represents $P < 0.01$ and *** represents $P < 0.001$.

<https://doi.org/10.1371/journal.pone.0283047.g003>

knockdown of ERRA (shERRA), were grown in serum-free media for 24 hrs and treated with tamoxifen for 5, 15, 30 and 60 min (Fig 4). As compared to control, MDA-MB-231 cells with reduced ERRA expression showed 2-fold upregulation of phosphorylation of p-ERK on Y204/187 (Fig 4A and 4B). This validates our previous findings and indicates that the effect of XCT-790 on ERK phosphorylation is due to its inhibition of ERRA. Furthermore, treatment of either MDA-MB-231 cells or cells with reduced expression of ERRA, showed that there is an inverse

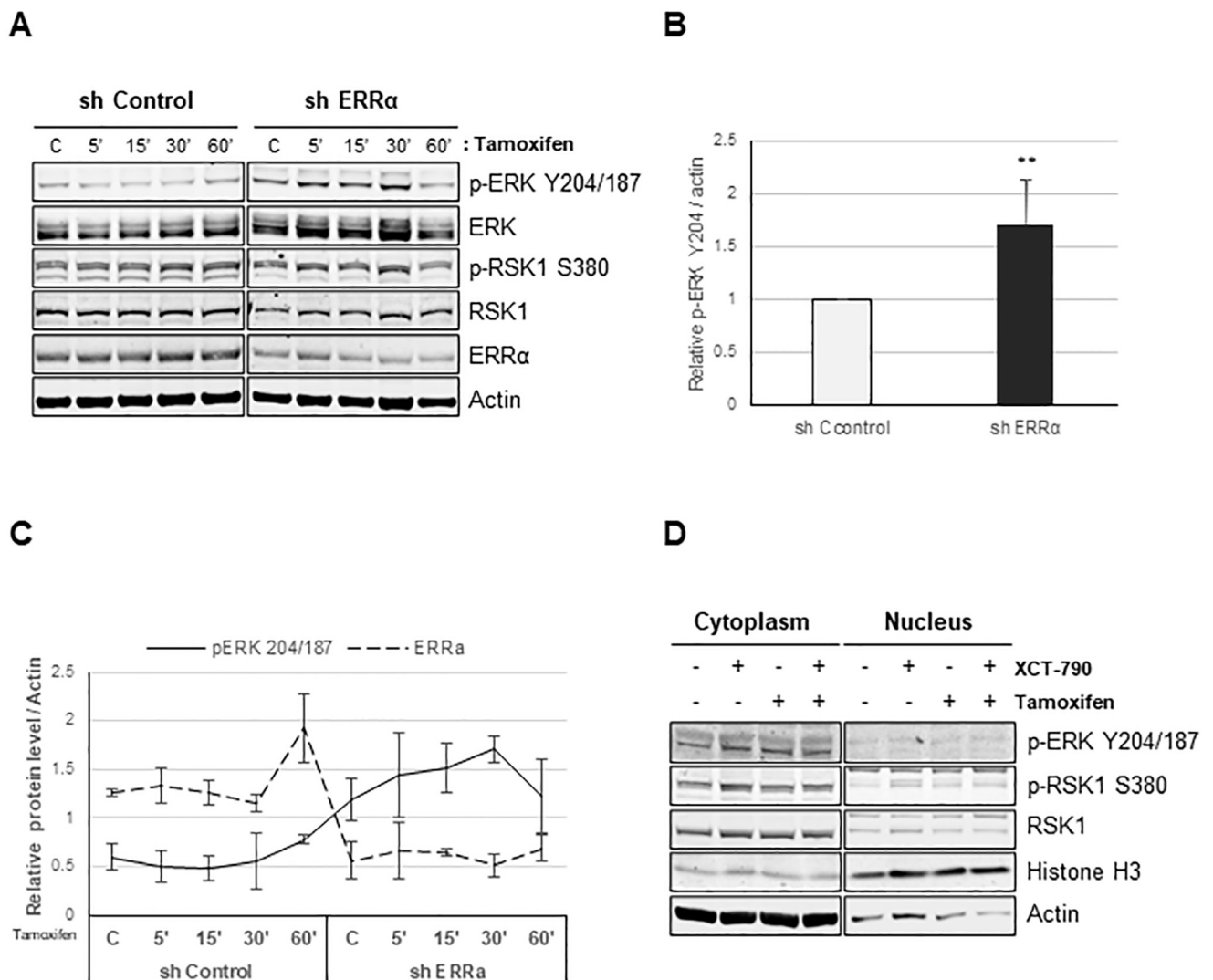


Fig 4. Tamoxifen potentiates phosphorylation of ERK on Y204/187 in the absence of ERRA. (A) sh Control and sh ERRA cells were treated with 100 nM of tamoxifen for 5, 15, 30, or 60 minutes. Cells were lysed as described in "Materials and Methods" and the indicated proteins were detected by immunoblot. (B) Relative levels of p-ERK Y204/187 normalized to actin, ** represents $P < 0.01$. (C) Relative levels of p-ERK Y204/187 and ERRA, normalized to actin from 'A'. (D) MDA-MB 231 cells were treated with 10 μ M XCT-790 and/or 100 nM tamoxifen for 30 minutes followed by lysis with NE-PER Nuclear Cytoplasmic extraction kit as described in 'Materials and Methods' and lysates from nuclear and cytoplasmic extractions were immunoblotted with the indicated antibodies.

<https://doi.org/10.1371/journal.pone.0283047.g004>

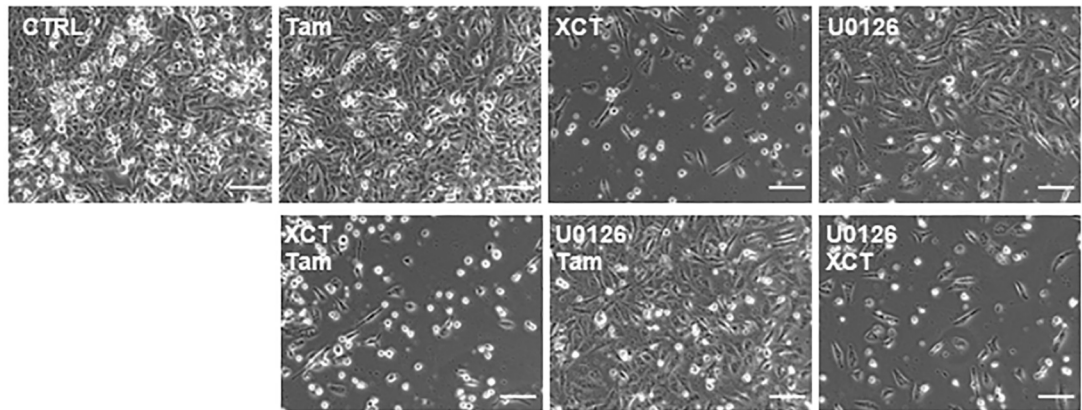
relationship between ERR α expression and phosphorylation of ERK on Y204/187, such that high ERR α expression in MDA-MB-231 cells is correlated with low p-ERK Y204/187 expression and reduced ERR α expression in sh-ERR α cells is correlated with increased phosphorylation of p-ERK on Y204/187 (Fig 4A and 4C). This finding further validates phosphoproteomic data and shows that inhibition of ERR α by XCT-790 as well as use of tamoxifen activate ERK signaling, and this has tremendously important implications for TNBC patients as we have identified a signaling pathway and a specific molecular target whose inhibition can be used therapeutically.

Since ERK is known to have both cytoplasmic as well nuclear functions, it is important to determine subcellular localization of p-ERK and its function. MDA-MB-231 cells were grown in serum-free media for 24 hrs, treated with tamoxifen and XCT-790, alone or in combination for 30 min, followed by preparation of nuclear and cytoplasmic fractions. As seen in Fig 4D, tamoxifen and XCT-790 treatment, alone or in combination, upregulated phosphorylation of ERK on Y204/187 specifically in the cytoplasm, and no p-ERK expression was detected in the nuclear fraction at this time point. Consistent with ERK's cytoplasmic function, its downstream target RSK1 was also phosphorylated on S380 upon tamoxifen as well as XCT-790 treatment, alone or in combination, and this was observed only in the cytoplasmic fraction and not in the nuclear fraction. The presence of histone H3 mainly in the nuclear fraction and presence of actin mainly in the cytoplasmic fraction served as technical control (Fig 4D).

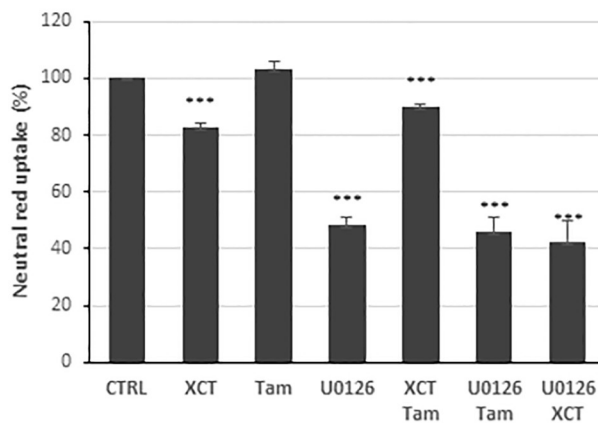
Since XCT-790 and tamoxifen treatments upregulate phosphorylation of ERK, this paves the way for investigating the use of MAPK inhibitors as a therapeutic strategy for TNBC patients. To that end, we investigated the effectiveness of U0126, a MEK1/2 inhibitor, in the context of TNBC cells. MDA-MB 231 cells were grown in serum free media and treated with 10 μ M XCT-790, 100 nM tamoxifen and 10 μ M U0126, alone or in combination (Fig 5). Following 48 hrs of treatment, cells were imaged with Keyence BZX-800 microscope under phase contrast (Fig 5A). Tamoxifen treatment alone did not have an effect on cell growth and density, however U0126 treatment and to a greater extent XCT-790 treatment showed a significant reduction in cell growth and density. Additionally, combination of tamoxifen together with XCT-790 as well as U0126 together with XCT-790 had a drastic and pronounced effect on cell density with very few cells attached. The attached cells were not healthy and appeared spindle-like or rounded up and majority of cells were floating dead cells. To quantify cell viability, relative uptake of neutral red dye by the lysosomes of live cells was measured. MDA-MB-231 cells were seeded in a 96-well plate in full serum media, treated with 10 μ M XCT-790, 100 nM tamoxifen and 10 μ M U0126, alone or in combination and neutral red assay was performed 6 days post treatment (Fig 5B). Consistent with previous observation, cells treated with XCT-790 had approximately 20% reduction in cell viability, while treatment of cells with U0126 alone or in combination with tamoxifen or XCT-790 had greater than 50% reduction in cell viability.

To further investigate whether the effect on cell viability is due to cell death, rather than inhibition of cell growth, expression level of cleaved-PARP fragment, a marker of apoptotic cell death was investigated (Fig 5C and 5D). MDA-MB-231 cells were grown in serum free media for 24 hrs and treated with 10 μ M XCT-790, 100 nM tamoxifen and 10 μ M U0126, alone or in combination for 24 hrs. As expected, U0126 treatment blocked activation of ERK signaling as seen via reduction of p-ERK Y204/187 and XCT-790 treatment reduced ERR α protein levels. Additionally, p-ERK Y204/187 and p-RSK1 S380 levels were upregulated upon treatment with XCT-790 and tamoxifen, validating previous data (Fig 5C). Most importantly, we observed statistically significant upregulation in apoptosis as measured by quantification of cleaved-PARP fragment (Fig 5D), indicated by the arrow (Fig 5C). The most notable increase in cleaved PARP levels was observed in samples treated with a combination of U0126 and XCT-790, which exhibited the greatest level of cleaved PARP when compared to cells treated with either U0126 or XCT-790, alone. This finding is very exciting as it indicates that the use

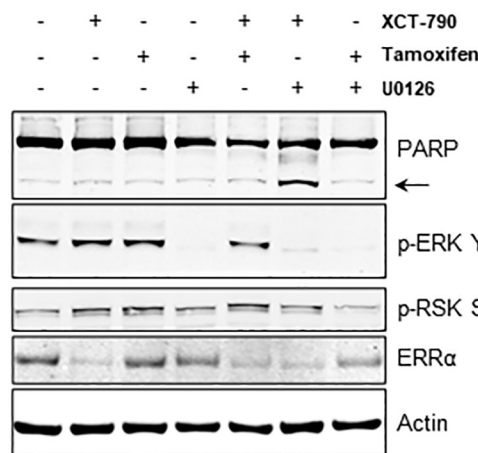
A



B



C



D

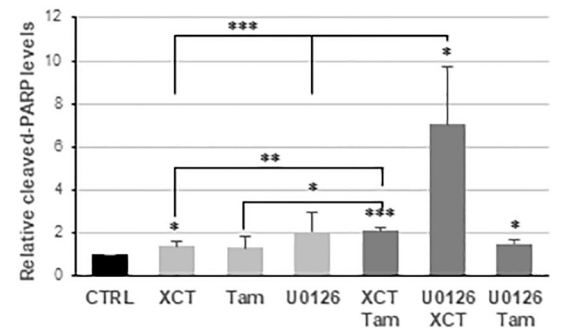


Fig 5. Inhibition of ERRA potentiates apoptotic effects of U0126 in TNBC cells. (A) MDA-MB-231 cells were serum starved for 24 hrs and treated with 10 μ M XCT-790, 100 nM tamoxifen, or 10 μ M U0126, alone or in combination for 48 hrs. Cells were imaged under 20x magnification using BZX-800 microscope from Keyence. Scale bar represents 100 μ m. (B) MDA-MB-231 cells were seeded in 96-well plate in complete DMEM media, supplemented with 10% FBS and treated with 10 μ M XCT-790, 100 nM tamoxifen, or 10 μ M U0126, alone or in combination for 6 days and cell viability was measured using Neutral Red cytotoxicity assay as described in "Materials and Methods". (C) MDA-MB-231 cells were serum starved for 24 hrs and treated with 10 μ M XCT-790, 100 nM tamoxifen, or 10 μ M U0126,

alone or in combination for 24 hrs as indicated. Cells were lysed as described in “Materials and Methods” and immunoblotted for indicated proteins. Arrow indicates cleaved PARP fragment. (D) Quantification of cleaved PARP fragment from “B” normalized to actin. * represents $P < 0.05$, ** represents $P < 0.01$ and *** represents $P < 0.001$.

<https://doi.org/10.1371/journal.pone.0283047.g005>

of MEK inhibitors together with inhibition of ERR α is effective at inducing apoptosis in TNBC cells and is a first indication of designing a targeted therapy for treatment of TNBC.

We subsequently wanted to examine whether such therapy is effective at inhibition migration and invasion of TNBC cells. To test the effect on cell motility, wound-healing assay was performed and quantified using MDA-MB-231 cells (Fig 6A and 6C). Though tamoxifen treatment alone did not have an effect on cell migration, treatment with either XCT-790 or U0126 had a statistically significant effect on inhibiting cell migration and this effect was also seen in combination therapy of XCT-790 with either tamoxifen or U0126. To test the effect on cell invasion, trans-well migration assay was performed and quantified using MDA-MB-231 cells (Fig 6B and 6D). Similar trend was observed in the trans-well migration assay as in the wound-healing assay. In particular, both XCT-790 and U0126 treatments had statistically significant inhibition on cell migration and this effect was maintained in all three combinations of treatments.

To verify that such therapy is beneficial to treatment of TNBC and is not unique to MDA-MB-231 cells, expression levels of ERR α and active signaling of MEK/ERK/RSK pathway were investigated in a panel of TNBC cells (Fig 7A). As expected, all of the tested TNBC cells express ERR α , but they also show active MEK/ERK/RSK signaling as indicated by phosphorylation of ERK on Y204/187 and RSK on S380. To identify the mechanism of XCT-790 action on ERK signaling, we wanted to see whether ERR α and ERK interact using co-immunoprecipitation assay using whole cell lysates. We confirmed that ERK and ERR α interact using MDA-MB 231 (Fig 7B) as well as high- ERR α expressing MDA-MB 436 (Fig 7C) cell lines.

Discussion

Despite significant strides that have been made in the development of treatments for hormone receptor positive breast cancer, progress in the treatment of TNBC has lagged behind, leaving patients with few treatment options. Results from previous studies identified a subset of patients with TNBC who have high ERR α expression and respond to tamoxifen treatment [25]. This finding prompted us to further investigate the role of ERR α in conferring tamoxifen sensitivity in TNBC tumors and to discover signaling pathways responsible for ERR α induced tamoxifen sensitivity, with the aim of identifying specific druggable target for the treatment of TNBC. In our study, we discovered that the MAPK signaling pathway is regulated by tamoxifen as well as ERR α and that attenuation of this signaling pathway may be a promising therapeutic strategy for the treatment of TNBC. Though the mechanism of tamoxifen action in TNBC cells is not clear, since ERR α and ER α can regulate a subset of common target genes, specifically ones with high relevance to breast tumor biology [35], it is possible that tamoxifen might have a similar mechanism of action on ERR α as it does on ER α . Of the targets we identified through phosphoproteomic analysis, MAPK1 phosphorylation at Y204/187 was particularly interesting as the MAPK pathway has been implicated in many processes associated with cancer progression including, tumor proliferation, invasion, metastasis, migration, and apoptosis [36, 37]. MAPK1 is part of a kinase signaling cascade that begins extracellularly with the EGFR receptor and cascades through a series of kinases including Ras, Raf, MEK, and ERK 1/2 consecutively [38]. ERK 2 is also known as MAPK1 and is a serine threonine kinase [39]. The identification of ERK as a target of ERR α and tamoxifen identifies an important target whose modulation should be further explored clinically as a therapy in TNBC.

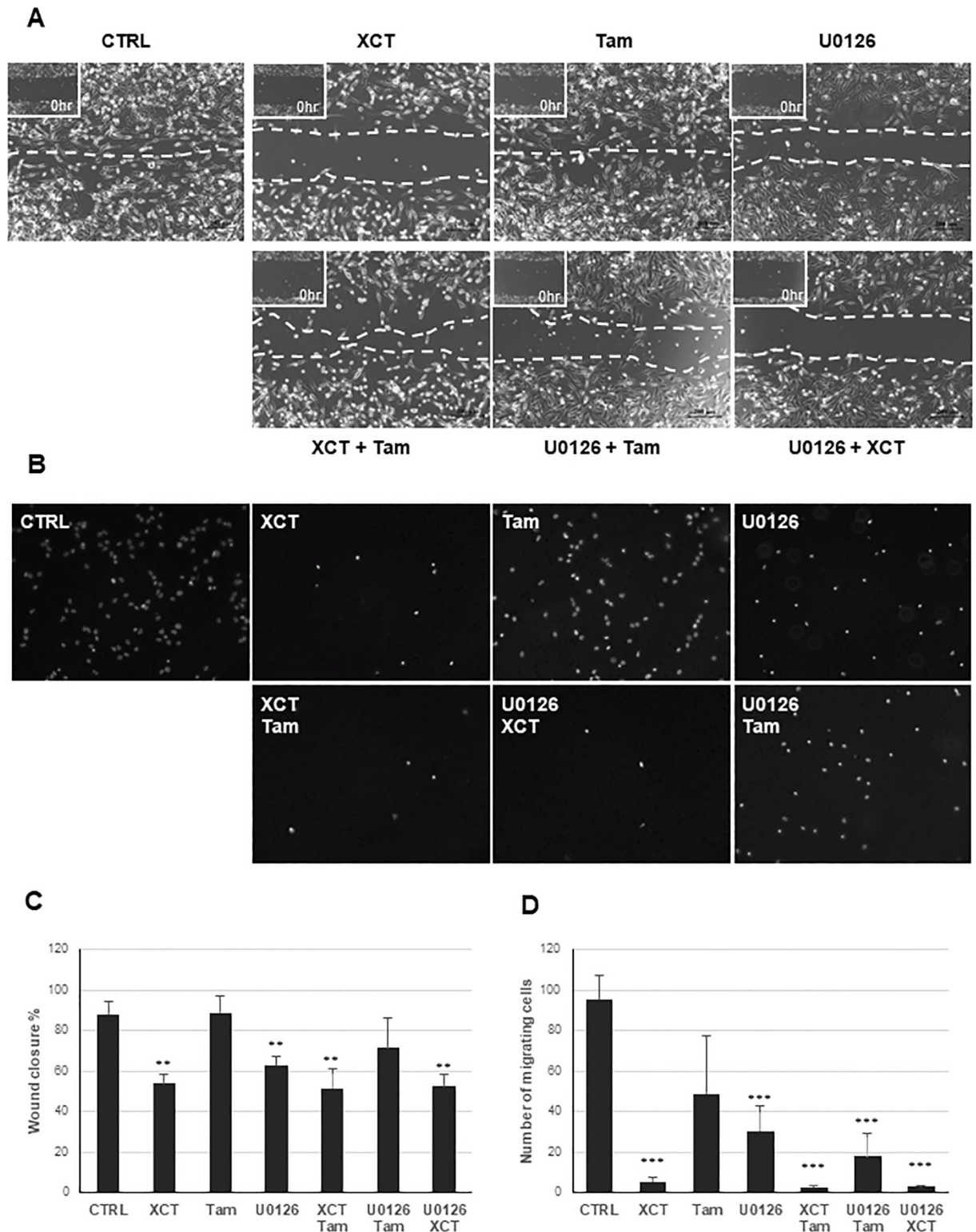


Fig 6. Inhibition of ERRA together with U0126 prevents cell migration and invasion in TNBC cells. (A) MDA-MB-231 cells were seeded in a 6-well plate in complete DMEM media and allowed to attach overnight. The following day cells were placed in reduced (1%) serum media and following 8–10 hrs of pretreatment with 10 μ M XCT-790, 100nM tamoxifen, or 10 μ M U0126, alone or in combination and wound/scratch was generated. Wound closure was measured 17 hrs post generation. (B) Cell migration/Boyden chamber assay was performed as described in “Materials and Methods”. Representative images of MDA-MB-231 cells stained with 4',6-diamidino-2-phenylindole (DAPI)

following 15 hrs migration assay are shown. (C) Quantification of the Wound Healing assay from (A) was performed and graphed using paired Student's t-test. * represents $P < 0.05$. ** represents $P < 0.01$. (D) Histogram representing the number of cells migrated relative to untreated control. * represents $P < 0.05$, ** represents $P < 0.01$ and *** represents $P < 0.001$.

<https://doi.org/10.1371/journal.pone.0283047.g006>

Further validation of the phosphoproteomic result with immunoblotting confirmed that XCT-790 as well as tamoxifen treatment led to an increase in ERK phosphorylation on Y204/187 as well as phosphorylation of the downstream kinase cascade. Our results show that ERR α directly binds to MAPK1, and through this interaction leads to modulation of MAPK1 phosphorylation on Y204/187 as well as downstream signaling. Since MAPK activation is known to support cellular survival, we hypothesized that this activation might be a compensatory cellular signal in response to treatment. Such compensatory responses have been previously described and have been implicated in the development of drug resistance [40]. Crosstalk from other pathways such as PI3K/Akt/mTOR or activation feedback loops within the Raf/MEK/ERK signaling pathway have been previously implicated in pro-survival compensatory mechanisms and drug resistance, thus encouraging further research into the use of drug combinations that act on multiple targets and disrupt the molecular compensatory mechanisms [37, 41, 42]. Though activation of Raf/MEK/ERK signaling is associated with tumor progression, it also identified an ERR α dependent target whose inhibition can be explored clinically for treatment of TNBC tumors.

Strategies to curb tumor progression through the inhibition of the MAPK pathway have been previously described and are currently used in the treatment of colon cancer and melanoma [43–53]. In breast cancer, preclinical studies described reduced tumor volume in xenograft models, induced cell cycle arrest, and increased apoptosis with the attenuation of the MAPK pathway [54, 55]. Though these results have yet to be validated in clinical trials, inhibition of EGFR in breast cancer was tested clinically due to evidence of EGFR overexpression in nearly half of TNBCs [43, 44]. Results from those trials were limited showing benefit only in certain subgroups of patients and clinical trials exploring the use of MEK inhibitors in breast cancers are currently underway. In our work, we showed that a combination of ERR α inverse agonist and MEK inhibition leads to statistically significant reduction in cell proliferation, upregulation of apoptosis as well as inhibition of cell migration and invasion.

TNBC is a highly aggressive and metastatic form of breast cancer with a poor prognosis and poor patient outcome. To date, we do not have a clear understanding of molecular pathways

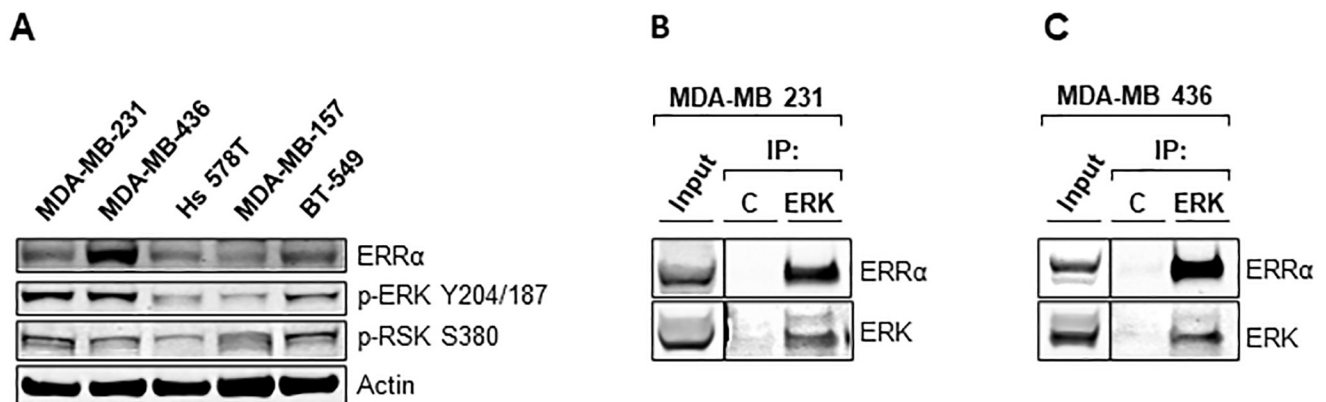


Fig 7. ERR α directly binds to ERK. (A) The represented TNBC cell lines were lysed as described in “Materials and Methods” and immunoblotted for the indicated proteins. (B) MDA-MB 231 cells were lysed and immunoprecipitated as described in “Materials and Methods” and proteins were detected by immunoblot. (C) MDA-MB 436 cells were lysed and immunoprecipitated as described in “Materials and Methods” and proteins were detected by immunoblot.

<https://doi.org/10.1371/journal.pone.0283047.g007>

that modulate cancer progression and therefore no targeted treatment therapies exist for TNBC patients. What is exciting and important is that we, for the first time, present data that show a direct link between ERRA and ERK signaling pathway. ERRA is a transcription factor that is highly expressed in TNBC and is associated with a more aggressive cancer and a poor outcome. We have shown that ERRA directly binds to ERK and modulates its phosphorylation on Y204/187 as well as downstream pathway activation, indicating that inhibitors of the MEK/ERK signaling pathway should be considered therapeutically for treatment of TNBC. As a proof of this concept, we showed that the use of MEK1/2 inhibitor alone or in combination with XCT-790 induces apoptosis as well as inhibits migration and invasion in TNBC cells. This is a highly exciting finding for TNBC patients and indicates that further investigation into clinical use of MEK inhibitors should be done for treatment of TNBC.

Supporting information

S1 Fig. Principal component analysis (PCA). Principal component analysis of protein abundance of MDA-MB 231 cells treated with tamoxifen, XCT-790 or tamoxifen plus XCT-790. (PDF)

S1 Table. All phosphoproteomic targets. (XLSX)

S2 Table. Phosphotargets with statistically significant changes in phosphorylation in at least one treatment condition ($P < 0.05$ in green). (XLSX)

S1 Raw images. (PDF)

Acknowledgments

We thank Dr. Marina Holz lab for sample preparation for phosphoproteomic analysis.

Author Contributions

Conceptualization: Anya Alayev.

Data curation: David Musheyev, Esther Miller, Natania Birnbaum, Elisheva Miller, Shoshana Erblich, Alyssa Schuck, Anya Alayev.

Formal analysis: David Musheyev, Esther Miller, Natania Birnbaum, Anya Alayev.

Funding acquisition: Anya Alayev.

Investigation: David Musheyev, Alyssa Schuck, Anya Alayev.

Methodology: Shoshana Erblich, Anya Alayev.

Writing – original draft: David Musheyev.

Writing – review & editing: David Musheyev, Alyssa Schuck, Anya Alayev.

References

1. Nagini S. Breast Cancer: Current Molecular Therapeutic Targets and New Players. *Anticancer Agents Med Chem.* 2017; 17(2):152–63. <https://doi.org/10.2174/1871520616666160502122724> PMID: 27137076

2. S RI, M Kd, F He, J A. Cancer Statistics, 2021. *CA Cancer J Clin.* 2021 Jan 12; 71(1):7–33. <https://doi.org/10.3322/caac.21654> PMID: 33433946
3. DeSantis CE, Ma J, Gaudet MM, Newman LA, Miller KD, Sauer AG, et al. Breast cancer statistics, 2019. *CA Cancer J Clin.* 2019; 69(6):438–51. <https://doi.org/10.3322/caac.21583> PMID: 31577379
4. Pfeiffer RM, Webb-Vargas Y, Wheeler W, Gail MH. Proportion of U.S. Trends in Breast Cancer Incidence Attributable to Long-term Changes in Risk Factor Distributions. *Cancer Epidemiol Prev Biomark.* 2018 Oct 1; 27(10):1214–22. <https://doi.org/10.1158/1055-9965.EPI-18-0098> PMID: 30068516
5. Howlader N, Cronin KA, Kurian AW, Andridge R. Differences in Breast Cancer Survival by Molecular Subtypes in the United States. *Cancer Epidemiol Prev Biomark.* 2018 Jun 1; 27(6):619–26. <https://doi.org/10.1158/1055-9965.EPI-17-0627> PMID: 29593010
6. Jiralerspong S, Goodwin PJ. Obesity and Breast Cancer Prognosis: Evidence, Challenges, and Opportunities. *J Clin Oncol.* 2016 Nov 7; 34(35):4203–16. <https://doi.org/10.1200/JCO.2016.68.4480> PMID: 27903149
7. Osborne CK, Yochmowitz MG, Knight WA, McGuire WL. The value of estrogen and progesterone receptors in the treatment of breast cancer. *Cancer.* 1980; 46(S12):2884–8. [https://doi.org/10.1002/1097-0142\(19801215\)46:12+<2884::aid-cnrcr2820461429>3.0.co;2-u](https://doi.org/10.1002/1097-0142(19801215)46:12+<2884::aid-cnrcr2820461429>3.0.co;2-u) PMID: 7448733
8. Burstein HJ. Systemic Therapy for Estrogen Receptor–Positive, HER2–Negative Breast Cancer. *N Engl J Med.* 2020 Dec 24; 383(26):2557–70. <https://doi.org/10.1056/NEJMra1307118> PMID: 33369357
9. Metzger-Filho O, Tutt A, de Azambuja E, Saini KS, Viale G, Loi S, et al. Dissecting the Heterogeneity of Triple–Negative Breast Cancer. *J Clin Oncol.* 2012 Mar 26; 30(15):1879–87. <https://doi.org/10.1200/JCO.2011.38.2010> PMID: 22454417
10. Lehmann BD, Bauer JA, Chen X, Sanders ME, Chakravarthy AB, Shyr Y, et al. Identification of human triple–negative breast cancer subtypes and preclinical models for selection of targeted therapies [Internet]. American Society for Clinical Investigation; 2011 [cited 2021 May 4]. Available from: <https://www.jco.org/articles/view/45014/pdf> <https://doi.org/10.1172/JCI45014> PMID: 21633166
11. Gupta GK, Collier AL, Lee D, Hofer RA, Zheleva V, Siewertsz van Reesema LL, et al. Perspectives on Triple–Negative Breast Cancer: Current Treatment Strategies, Unmet Needs, and Potential Targets for Future Therapies. *Cancers.* 2020 Sep; 12(9):2392. <https://doi.org/10.3390/cancers12092392> PMID: 32846967
12. Vagia E, Mahalingam D, Cristofanilli M. The Landscape of Targeted Therapies in TNBC. *Cancers* [Internet]. 2020 Apr 8 [cited 2021 Apr 21]; 12(4). Available from: <https://www.ncbi.nlm.nih.gov/pmc/articles/PMC7226210/> <https://doi.org/10.3390/cancers12040916> PMID: 32276534
13. De Marchi T, Foekens JA, Umar A, Martens JWM. Endocrine therapy resistance in estrogen receptor (ER)–positive breast cancer. *Drug Discov Today.* 2016 Jul; 21(7):1181–8. <https://doi.org/10.1016/j.drudis.2016.05.012> PMID: 27233379
14. Johnston SRD. New Strategies in Estrogen Receptor–Positive Breast Cancer. *Clin Cancer Res.* 2010 Apr 1; 16(7):1979–87. <https://doi.org/10.1158/1078-0432.CCR-09-1823> PMID: 20332324
15. Osborne CK. Tamoxifen in the Treatment of Breast Cancer. *N Engl J Med.* 1998 Nov 26; 339(22):1609–18. <https://doi.org/10.1056/NEJM199811263392207> PMID: 9828250
16. Herynk MH, Fuqua SAW. Estrogen Receptor Mutations in Human Disease. *Endocr Rev.* 2004 Dec 1; 25(6):869–98. <https://doi.org/10.1210/er.2003-0010> PMID: 15583021
17. Fuqua SA, Chamness GC, McGuire WL. Estrogen receptor mutations in breast cancer. *J Cell Biochem.* 1993 Feb; 51(2):135–9. <https://doi.org/10.1002/jcb.240510204> PMID: 8440747
18. Čufer T. Reducing the risk of late recurrence in hormone–responsive breast cancer. *Ann Oncol.* 2007 Sep 1; 18:viii18–25. <https://doi.org/10.1093/annonc/mdm262> PMID: 17890210
19. Prat A, Parker JS, Karginova O, Fan C, Livasy C, Herschkowitz JI, et al. Phenotypic and molecular characterization of the claudin–low intrinsic subtype of breast cancer. *Breast Cancer Res.* 2010 Sep 2; 12(5):R68. <https://doi.org/10.1186/bcr2635> PMID: 20813035
20. Liedtke C, Mazouni C, Hess KR, André F, Tordai A, Mejia JA, et al. Response to Neoadjuvant Therapy and Long–Term Survival in Patients With Triple–Negative Breast Cancer. *J Clin Oncol* [Internet]. 2016 Sep 22 [cited 2021 Jul 20]; Available from: <https://ascopubs.org/doi/pdf/10.1200/JCO.2007.14.4147>
21. Mayer EL, Burstein HJ. Chemotherapy for Triple–Negative Breast Cancer: Is More Better? *J Clin Oncol* [Internet]. 2016 Aug 22 [cited 2021 May 4]; Available from: <https://ascopubs.org/doi/pdf/10.1200/JCO.2016.68.4068> PMID: 27551109
22. Rouzier R, Perou CM, Symmans WF, Ibrahim N, Cristofanilli M, Anderson K, et al. Breast Cancer Molecular Subtypes Respond Differently to Preoperative Chemotherapy. *Clin Cancer Res.* 2005 Aug 15; 11(16):5678–85. <https://doi.org/10.1158/1078-0432.CCR-04-2421> PMID: 16115903

23. Schirmacher V. From chemotherapy to biological therapy: A review of novel concepts to reduce the side effects of systemic cancer treatment (Review). *Int J Oncol*. 2019 Feb 1; 54(2):407–19. <https://doi.org/10.3892/ijo.2018.4661> PMID: 30570109
24. Berman AY, Manna S, Schwartz NS, Katz YE, Sun Y, Behrmann CA, et al. ERRA regulates the growth of triple-negative breast cancer cells via S6K1-dependent mechanism. *Signal Transduct Target Ther*. 2017; 2:e17035.
25. Manna S, Bostner J, Sun Y, Miller LD, Alayev A, Schwartz NS, et al. ERRA is a marker of tamoxifen response and survival in triple-negative breast cancer. *Clin Cancer Res Off J Am Assoc Cancer Res*. 2016 Mar 15; 22(6):1421–31.
26. Ariazi EA, Clark GM, Mertz JE. Estrogen-related Receptor α and Estrogen-related Receptor γ Associate with Unfavorable and Favorable Biomarkers, Respectively, in Human Breast Cancer. *Cancer Res*. 2002 Nov 15; 62(22):6510–8.
27. Jarzabek K, Koda M, Kozlowski L, Sulkowski S, Kottler ML, Wolczynski S. The significance of the expression of ERRA as a potential biomarker in breast cancer. *J Steroid Biochem Mol Biol*. 2009 Jan 1; 113(1):127–33.
28. Villena JA, Kralli A. ERRA: a metabolic function for the oldest orphan. *Trends Endocrinol Metab*. 2008 Oct 1; 19(8):269–76.
29. Huss JM, Garbacz WG, Xie W. Constitutive activities of estrogen-related receptors: Transcriptional regulation of metabolism by the ERR pathways in health and disease. *Biochim Biophys Acta BBA—Mol Basis Dis*. 2015 Sep 1; 1852(9):1912–27. <https://doi.org/10.1016/j.bbadis.2015.06.016> PMID: 26115970
30. Bianco S, Sailland J, Vanacker JM. ERRs and cancers: Effects on metabolism and on proliferation and migration capacities. *J Steroid Biochem Mol Biol*. 2012 Jul 1; 130(3):180–5. <https://doi.org/10.1016/j.jsbmb.2011.03.014> PMID: 21414406
31. Ranhotra HS. The estrogen-related receptors in metabolism and cancer: newer insights. *J Recept Signal Transduct*. 2018 Mar 4; 38(2):95–100. <https://doi.org/10.1080/10799893.2018.1456552> PMID: 29619877
32. Casaburi I, Chimento A, De Luca A, Nocito M, Sculco S, Avena P, et al. Cholesterol as an Endogenous ERRA Agonist: A New Perspective to Cancer Treatment. *Front Endocrinol*. 2018; 9:525.
33. Busch BB, Stevens WC, Martin R, Ordentlich P, Zhou S, Sapp DW, et al. Identification of a selective inverse agonist for the orphan nuclear receptor estrogen-related receptor alpha. *J Med Chem*. 2004 Nov 4; 47(23):5593–6. <https://doi.org/10.1021/jm049334f> PMID: 15509154
34. Alayev A, Holz MK. mTOR signaling for biological control and cancer. *J Cell Physiol*. 2013 Aug; 228(8):1658–64. <https://doi.org/10.1002/jcp.24351> PMID: 23460185
35. Deblois G, Hall JA, Perry MC, Laganière J, Ghahremani M, Park M, et al. Genome-Wide Identification of Direct Target Genes Implicates Estrogen-Related Receptor α as a Determinant of Breast Cancer Heterogeneity. *Cancer Res*. 2009 Jul 29; 69(15):6149–57.
36. Maurer G, Tarkowski B, Baccarini M. Raf kinases in cancer—roles and therapeutic opportunities. *Oncogene*. 2011 Aug; 30(32):3477–88. <https://doi.org/10.1038/onc.2011.160> PMID: 21577205
37. Braicu C, Buse M, Busuioc C, Drula R, Gulei D, Raduly L, et al. A Comprehensive Review on MAPK: A Promising Therapeutic Target in Cancer. *Cancers*. 2019 Oct 22; 11(10):E1618. <https://doi.org/10.3390/cancers11101618> PMID: 31652660
38. Roberts PJ, Der CJ. Targeting the Raf-MEK-ERK mitogen-activated protein kinase cascade for the treatment of cancer. *Oncogene*. 2007 May; 26(22):3291–310. <https://doi.org/10.1038/sj.onc.1210422> PMID: 17496923
39. Wortzel I, Seger R. The ERK Cascade: Distinct Functions within Various Subcellular Organelles. *Genes Cancer*. 2011 Mar 1; 2(3):195–209. <https://doi.org/10.1177/1947601911407328> PMID: 21779493
40. Trusolino L, Bertotti A. Compensatory Pathways in Oncogenic Kinase Signaling and Resistance to Targeted Therapies: Six Degrees of Separation. *Cancer Discov*. 2012 Oct 1; 2(10):876–80. <https://doi.org/10.1158/2159-8290.CD-12-0400> PMID: 23071031
41. De Luca A, Maiello MR, D'Alessio A, Pergameno M, Normanno N. The RAS/RAF/MEK/ERK and the PI3K/AKT signalling pathways: role in cancer pathogenesis and implications for therapeutic approaches. *Expert Opin Ther Targets*. 2012 Apr 1; 16(sup2):S17–27. <https://doi.org/10.1517/14728222.2011.639361> PMID: 22443084
42. You KS, Yi YW, Cho J, Seong YS. Dual Inhibition of AKT and MEK Pathways Potentiates the Anti-Cancer Effect of Gefitinib in Triple-Negative Breast Cancer Cells. *Cancers*. 2021 Jan; 13(6):1205. <https://doi.org/10.3390/cancers13061205> PMID: 33801977
43. Di Leo A, Gomez HL, Aziz Z, Zvirbule Z, Bines J, Arbushites MC, et al. Phase III, double-blind, randomized study comparing lapatinib plus paclitaxel with placebo plus paclitaxel as first-line treatment for

- metastatic breast cancer. *J Clin Oncol Off J Am Soc Clin Oncol*. 2008 Dec 1; 26(34):5544–52. <https://doi.org/10.1200/JCO.2008.16.2578> PMID: 18955454
44. Finn RS, Press MF, Dering J, Arbushites M, Koehler M, Oliva C, et al. Estrogen receptor, progesterone receptor, human epidermal growth factor receptor 2 (HER2), and epidermal growth factor receptor expression and benefit from lapatinib in a randomized trial of paclitaxel with lapatinib or placebo as first-line treatment in HER2-negative or unknown metastatic breast cancer. *J Clin Oncol Off J Am Soc Clin Oncol*. 2009 Aug 20; 27(24):3908–15. <https://doi.org/10.1200/JCO.2008.18.1925> PMID: 19620495
 45. Baselga J, Gómez P, Greil R, Braga S, Climent MA, Wardley AM, et al. Randomized phase II study of the anti-epidermal growth factor receptor monoclonal antibody cetuximab with cisplatin versus cisplatin alone in patients with metastatic triple-negative breast cancer. *J Clin Oncol Off J Am Soc Clin Oncol*. 2013 Jul 10; 31(20):2586–92. <https://doi.org/10.1200/JCO.2012.46.2408> PMID: 23733761
 46. Nabholz JM, Chalabi N, Radosevic-Robin N, Dauplat MM, Mouret-Reynier MA, Van Praagh I, et al. Multicentric neoadjuvant pilot Phase II study of cetuximab combined with docetaxel in operable triple negative breast cancer. *Int J Cancer*. 2016 May 1; 138(9):2274–80. <https://doi.org/10.1002/ijc.29952> PMID: 26649807
 47. Yardley DA, Ward PJ, Daniel BR, Eakle JF, Lamar RE, Lane CM, et al. Panitumumab, Gemcitabine, and Carboplatin as Treatment for Women With Metastatic Triple-Negative Breast Cancer: A Sarah Cannon Research Institute Phase II Trial. *Clin Breast Cancer*. 2016 Oct; 16(5):349–55. <https://doi.org/10.1016/j.clbc.2016.05.006> PMID: 27340049
 48. LoRusso PM, Krishnamurthi SS, Rinehart JJ, Nabell LM, Malburg L, Chapman PB, et al. Phase I Pharmacokinetic and Pharmacodynamic Study of the Oral MAPK/ERK Kinase Inhibitor PD-0325901 in Patients with Advanced Cancers. *Clin Cancer Res*. 2010 Mar 15; 16(6):1924–37. <https://doi.org/10.1158/1078-0432.CCR-09-1883> PMID: 20215549
 49. Rinehart J, Adjei AA, LoRusso PM, Waterhouse D, Hecht JR, Natale RB, et al. Multicenter Phase II Study of the Oral MEK Inhibitor, CI-1040, in Patients With Advanced Non-Small-Cell Lung, Breast, Colon, and Pancreatic Cancer. *J Clin Oncol*. 2004 Nov 15; 22(22):4456–62. <https://doi.org/10.1200/JCO.2004.01.185> PMID: 15483017
 50. Hainsworth JD, Cebotaru CL, Kanarev V, Ciuleanu TE, Damyranov D, Stella P, et al. A Phase II, Open-Label, Randomized Study to Assess the Efficacy and Safety of AZD6244 (ARRY-142886) Versus Pemetrexed in Patients with Non-small Cell Lung Cancer Who Have Failed One or Two Prior Chemotherapeutic Regimens. *J Thorac Oncol*. 2010 Oct 1; 5(10):1630–6. <https://doi.org/10.1097/JTO.0b013e3181e8b3a3> PMID: 20802351
 51. Flaherty KT, Infante JR, Daud A, Gonzalez R, Kefford RF, Sosman J, et al. Combined BRAF and MEK Inhibition in Melanoma with BRAF V600 Mutations. *N Engl J Med*. 2012 Nov 1; 367(18):1694–703. <https://doi.org/10.1056/NEJMoa1210093> PMID: 23020132
 52. Burotto M, Chiou VL, Lee JM, Kohn EC. The MAPK pathway across different malignancies: A new perspective. *Cancer*. 2014 Nov 15; 120(22):3446–56. <https://doi.org/10.1002/ncr.28864> PMID: 24948110
 53. Zhou S, Xia H, Xu H, Tang Q, Nie Y, yong Gong Q, et al. ERRA suppression enhances the cytotoxicity of the MEK inhibitor trametinib against colon cancer cells. *J Exp Clin Cancer Res*. 2018 Dec; 37(1):1–14.
 54. Hoeflich KP, O'Brien C, Boyd Z, Cavet G, Guerrero S, Jung K, et al. In vivo Antitumor Activity of MEK and Phosphatidylinositol 3-Kinase Inhibitors in Basal-Like Breast Cancer Models. *Clin Cancer Res*. 2009 Jul 15; 15(14):4649–64. <https://doi.org/10.1158/1078-0432.CCR-09-0317> PMID: 19567590
 55. Maiello MR, D'Alessio A, Bevilacqua S, Gallo M, Normanno N, D Luca A. EGFR and MEK Blockade in Triple Negative Breast Cancer Cells. *J Cell Biochem*. 2015; 116(12):2778–85. <https://doi.org/10.1002/jcb.25220> PMID: 25959272